INTERNATIONAL JOURNAL FOR NUMERICAL AND ANALYTICAL METHODS IN GEOMECHANICS, VOL. 20, 253–273 (1996)

SILENT BOUNDARY CONDITIONS FOR WAVE PROPAGATION IN SATURATED POROUS MEDIA

A. GAJO

Dipartimento di Meccanica Strutturale e Progettazione Automatica, Università di Trento, Via Mesiano, 77, 38050 Trento, Italy

A. SAETTA

Dipartimento di Costruzione dell'Architettura, Istituto Universitario di Architettura di Venezia, Tolentini, 191, 30135 Venezia, Italy

AND

R. VITALIANI

Istituto di Scienza e Tecnica delle Costruzioni, Facoltà di Ingegneria, Università di Padova, Via Marzolo, 9, 35131 Padova, Italy

SUMMARY

Wave propagation both in one- and in two-dimensional saturated elastic porous media is analysed by means of a two-field finite element model with silent boundaries. An extension of the elastic 'multidirectional' transmitting boundary to two-phase media is developed to simulate the silent boundary condition. The theoretical assessment and the numerical formulation of the first-order silent boundary technique is presented in detail. Some examples are used to demonstrate the reliability of the first-order method, especially for problems with plane and axisymmetric waves having various angles of incidence. Finally, the wave propagation along a pile shaft is presented, to simulate a common non-destructive dynamic pile test.

KEY WORDS: elastic porous media; wave propagation; first-order silent boundary technique

1. INTRODUCTION

An understanding of the dynamic behaviour of saturated elastic porous media is of great concern in many fields, such as seismology, earthquake engineering and soil dynamics.

In recent years, extensive use has been made of the finite element method in solving dynamic problems, because of its versatility and reliability in all fields of application. In numerical simulations, attention is usually restricted to a finite region. When the spatial domain of the problem is unbounded, then an artificial boundary condition is needed to make the computational domain finite. The appropriate artificial boundary condition for different wave problems is an important issue, since it must be designed to avoid the reflection of waves radiating toward infinity in the finite computational domain. Such boundary conditions have been referred to by a variety of names, such as absorbing, silent, anechoic, non-reflecting, transmitting, radiating, transparent and one-way boundary conditions. The term 'silent boundary' will be used here.

Silent boundaries have been proposed for both scalar (acoustic) and vectorial (elastic) wave equations. An interesting review by Givoli[1] summarizes some of these methods. The present

CCC 0363–9061/96/040253–21

Received 8 August 1994
Revised 29 August 1995

discussion will be restricted to the methods developed for the elastic wave equation. First the silent boundary for one-phase media will be reviewed, then its applicability to saturated porous media will be discussed.

For one-phase media, the exact exterior solution, which usually takes the form of exterior boundary integrals and which can be linked to the finite element computational grid (Zienkiewicz *et al.*[2]), has been formulated. Boundary elements and hybrid methods of finite and boundary elements have also frequently been used (see, for instance, References 3–5). Unfortunately such methods, which have been mainly applied to linear, isotropic, homogeneous materials, combine many boundary points, which is why they are defined as being 'non-local in space'. Moreover, the boundary integral method leads to non-symmetric matrices and is properly formulated in the frequency domain (i.e., it is also 'non-local in time') so it cannot be used directly with time-step integration techniques.[6] For an extension of the boundary element method to time-dependent problems, see Kawase[7] for example, who used the discrete wave number method, and Givoli[8], who applied a method based on an integral formulation to equations of motion discretized in time. Research on silent boundary methods which are local in time and in space is still an important issue, because such methods can easily be implemented and employed to study non-linear problems using standard time-step integration methods.

The first local silent boundary was proposed by Lysmer and Kuhlemeyer[9] and later improved by White *et al.*[10] This method is based on applying viscous damping forces along the boundary and is, therefore, referred to as a viscous boundary. This kind of silent boundary has been judged as not entirely satisfactory for certain applications. For a discussion of the errors induced by using the viscous boundary, see References 11 and 12.

Clayton and Engquist[13] extended the so-called para-axial boundary of Engquist and Majda[14] so as to deal with elastic wave propagation. This method is based on differential operators which satisfy the condition of only outgoing waves. While these differential operators may be of a high order, the para-axial boundary of the first order is identical to the viscous boundary. This method is most convenient for finite difference applications,[6] because a numerical technique called 'upwind' by Hughes[15] is needed for finite element applications.[12] Higher-order differential operators may lead to numerical instability, however.[12,16,17]

The silent boundary condition formulated by Higdom,[18,19] based on a series of first-order differential operators, may be considered a generalization of the higher-order differential operators of Engquist and Majda.[14] This boundary gives perfect absorption at certain angles of incidence and is thus called a multidirectional boundary. It also has the advantage of avoiding tangential derivatives at the boundary so that the implementation near a corner is straightforward.

A silent boundary method which related to the concept of para-axial method but avoided the numerical difficulties of the latter is the scheme proposed by Liao and Wong.[20] This method is also related to the space–time extrapolation scheme proposed by Higdom,[21] since both methods deal with difference equations. These methods are well suited to finite element applications and are based on predicting the motion at the boundary by extrapolating the motion at points in the neighbourhood of the boundary, which is why they are called extrapolation boundaries. An analysis of the numerical stability of the silent boundary proposed by Liao and Wong[20] can be found in Liao and Liu.[22] An improvement in this method has recently been published by Peng and Toksoz.[23]

A completely different method is the scheme originally proposed by Smith[24] and modified by Cundall.[25] This method is based on averaging the solutions of two complementary problems, one involving a fixed and the other a free boundary condition. The efficiency of the method, as modified by Cundall,[25] is comparable with that of the viscous boundary.[6]

Finally, silent boundaries have been obtained by using periodic infinite elements.[26] Periodic infinite elements are an extension of the infinite elements originally proposed for static problems to include periodic effects. This is achieved through the wave number of the outgoing wave, so these methods are frequency-dependent. Among the various infinite elements, the mapped kind appears to be the most accurate.[27] In elastic wave propagation problems, there are at least two kinds of wave and consequent wave numbers. It is also well known that further guided waves exist near an interface between two media, or near a free surface. Hence it is not clear which wave number should be assigned to the periodic infinite elements. Chow and Smith[28] arbitrarily assumed that the vertical component is related to the S-wave and the horizontal component to the P-wave.

In the field of the dynamics of saturated porous media, no silent boundary method for time-dependent problems has been proposed as yet. Only an application for time-harmonic problems has recently been published by Degrande and De Roeck.[29,30]

It is well known that saturated porous media are idealized by two phases, i.e. the elastic skeleton and the compressible pore fluid. These two phases are coupled at three levels, which are the inertial, viscous and mechanical levels. Inertial and mechanical couplings involve the propagation of two longitudinal waves (P1 and P2) and one rotational wave (S), whereas viscous coupling makes wave propagation dispersive. If permeability is low, or if the content in high frequencies of the problem to be analysed is low, viscous coupling may completely damp out the slowest longitudinal waves[31–34] and make the two-phase medium behave as a one-phase medium. Due to the presence of three kinds of body wave and to difficulties in choosing the right wave number, periodic infinite elements may not be directly applied to saturated porous media. Similarly, viscous para-axial, and multidirectional boundaries are not immediately suitable for such media, due to the coupled characteristics. None of the above-mentioned silent boundaries can therefore be directly applied to elastic wave propagation in saturated porous media. Only the boundary integral method can be used in saturated porous media, as Cheng *et al.*[35] did for harmonic wave propagation. It is worth mentioning that the time domain integral equation derived by Chen,[36] paves the way for implementing the boundary element method in the time domain. Unfortunately, this solution is based on the approximate expression of the velocity of propagation.

Kausel[6] has shown that the aforesaid methods, with the exception of the boundary integral and the periodic infinite elements, are all mathematically related and their efficiency for one-phase media is therefore comparable. The multidirectional boundary is the most general and its numerical stability for one-phase media has been demonstrated by Higdom.[18] In particular, the first-order form of the multidirectional boundary, i.e., the viscous boundary, is the easiest to implement, which explains our interest in developing an extension of the multidirectional boundary to saturated porous media for time-dependent problems. The objective is achieved here by first developing a set of first-order differential equations which allow the propagation of elastic waves travelling only in a single direction; higher-order multidirectional boundaries are thus obtained by using the same generalizations proposed by Higdom[18,19] for one-phase media. The present method was developed with reference to u–U formulation, though it can easily be extended to other two- and three-field formulations (i.e. u–w and u–p–U).[37–39]

The first-order silent boundary results from the combination of a line of fictitious dashpots, linked to both the absolute and the relative velocities of the two phases, and can be viewed as an extension of the viscous method to two-phase media. As in the viscous method, the fictitious dashpots do not depend on the frequencies of the transmitted waves. The cases of vanishingly small and infinitely large viscous coupling, corresponding, respectively, to a very high permeability and high-frequency content, and to a low permeability and low-frequency content, are studied.

A careful theoretical evaluation is made of the behaviour of the proposed method in an unbounded two-dimensional homogeneous poroelastic environment. This method requires only negligible effort and computational cost in the u–U finite element procedure developed by the authors[39] to solve some practical wave propagation problems, both in one and in two dimensions. Finally, a soil–pile interaction problem is studied to simulate a non-destructive dynamic pile test.

2. FIELD EQUATIONS

Starting from the Biot's well-known equations of motion for small strain of saturated linear elastic isotropic porous media,[31-34] by using a linear constitutive relationship and using a u–U formulation,[37-39] the following differential equations are obtained

$$\sigma''_{ji,j} - (\alpha - n)p_{,j}\delta_{ij} + (1-n)\rho_s b_i - (1-n)\rho_s \ddot{u}_i - \rho_a(\ddot{u}_i - \ddot{U}_i) - \frac{n^2}{k}(\dot{u}_i - \dot{U}_i) = 0$$

$$-np_{,i} + n\rho_f b_i - n\rho_f \ddot{U}_i - \rho_a(\ddot{U}_i - \ddot{u}_i) - \frac{n^2}{k}(\dot{U}_i - \dot{u}_i) = 0 \tag{1}$$

where u_i and U_i are, respectively, the absolute displacements of the solid skeleton and pore fluid, n is the porosity, $\alpha = 1 - K/K_s$, with K and K_s the bulk moduli of solid skeleton and solid grains, respectively, ρ_s and ρ_f are, respectively, the densities of the solid grains and pore fluid, ρ_a is the added mass, k is related to the coefficient of permeability, b_i are the body forces per unit of mass and

$$\sigma''_{ij} = D_{ijkl}\varepsilon_{kl}$$

$$-p = (\alpha - n)Q\varepsilon_{ii} + nQU_{i,i} \tag{2}$$

where D_{ijkl} is the quartic tensor of the solid skeleton's elastic constants, $1/Q = n/K_f + (\alpha - n)/K_s$, and K_f is the bulk modulus of the pore fluid.

3. THEORY OF SILENT BOUNDARY CONDITIONS

The explicit derivation of silent boundary conditions is only carried out for the extreme values of permeability: $k = \infty$ and $k = 0$. For a given finite value of permeability, these conditions refer to the propagation of high- and low-frequency pulses, respectively. In the first case (high-frequency pulses), viscous coupling is low and there are two longitudinal and one rotational wave; in the second case (low-frequency pulses), the porous medium practically behaves as a one-phase medium and only one longitudinal and one rotational wave exist.[31-34]. For the intermediate values of permeability and frequency content, wave propagation is dispersive, i.e., higher frequencies are faster but they are more heavily damped out.[40] The transition between low and high viscous coupling behaviour extends over quite a narrow range of value of permeability, travel length and frequency content of the driving pulse.[41]

The fact that only the extreme values of permeability and frequency are taken into account need not cause particular concern, because the difference in the longitudinal and rotational wave velocities between the two extreme cases is quite small, and the spurious reflections given by using one of the two extreme types of condition to study a problem with intermediate values of permeability and frequency are even smaller, as we shall see.

For many practical applications, moreover, knowing the permeability, the travel length and the frequency content of the transient event, enables a prediction of whether the propagation occurs with two-phase or one-phase characteristics,[41] so the most suitable type of silent boundary condition can be selected.

The theoretical analysis is limited to longitudinal waves, because rotational wave propagation is not coupled and the ordinary theory of viscous silent boundary conditions can be applied. The silent boundary condition for two-phase media wave propagation problems is obtained using the one-dimensional hypothesis, both for $k = \infty$ and $k = 0$. The next section analyses the reliability of this method, developed for one-dimensional propagation. for the the case of two-dimensional propagation. Assuming one-dimensional propagation along the x_1 direction enables the index notation to be dropped (i.e. $x = x_1$, $u = u_1$ and $U = U_1$).

For $k = \infty$, i.e., for a low viscous coupling, which is typical of a high coefficient of permeability as well as of high frequencies, and for null body forces ($b_1 = 0$), the equations of motion become:

$$\begin{aligned} \rho_{11}u_{tt} + \rho_{12}U_{tt} &= c_{11}u_{xx} + c_{12}U_{xx} \\ \rho_{12}u_{tt} + \rho_{22}U_{tt} &= c_{12}u_{xx} + c_{22}U_{xx} \end{aligned} \tag{3}$$

where u_{tt}, U_{tt}, u_{xx} and U_{xx} are the second derivatives and

$$c_{11} = \lambda + 2\mu + (\alpha - n)^2 Q, \qquad c_{12} = n(\alpha - n)Q, \qquad c_{22} = n^2 Q$$

$$\rho_{11} = (1 - n)\rho_s + (\tau - 1)n\rho_f, \qquad \rho_{12} = -(\tau - 1)n\rho_f, \qquad \rho_{22} = n\rho_f + (\tau - 1)n\rho_f \tag{4}$$

where λ and μ are the Lamè constants. Such a system of differential equations can be written in matrix notation as

$$\mathbf{M}\mathbf{X}_{xx} - \mathbf{K}\mathbf{X}_{tt} = \mathbf{0} \tag{5}$$

where $\mathbf{X}^T = [u, U]$ and may be solved using the Laplace transform. This leads to an eigenvalue problem, with the following characteristic equation:[42]

$$(\rho_1\rho_2 + \rho_1\rho_a + \rho_2\rho_a)v^4 - [(c_{11} + 2c_{12} + c_{22})\rho_a + c_{22}\rho_1 + c_{11}\rho_2]v^2 + (c_{11}c_{22} - c_{12}^2) = 0 \tag{6}$$

the solutions of which gives the propagation velocities v_1 and v_2. The associated eigenvectors are $\bar{\mathbf{X}}_1^T = [1, \beta_1]$ and $\bar{\mathbf{X}}_2^T = [1, \beta_2]$, where β_1 and β_2 represent the ratio between the fluid and solid wave amplitudes, for the longitudinal wave of the first and second kind, respectively, and can be expressed as

$$\begin{aligned} \beta_1 &= -\frac{\rho_{11}v_1^2 - c_{11}}{\rho_{12}v_1^2 - c_{12}} \\ \beta_2 &= -\frac{\rho_{11}v_2^2 - c_{11}}{\rho_{12}v_2^2 - c_{12}} \end{aligned} \tag{7}$$

In the derivation of the silent boundary condition, a system of partial differential equations is needed, which allows the waves to travel only in the positive x-direction. A first-order equation system that satisfies such a condition is as follows:

$$\begin{aligned} \rho_1 u_t + \rho_2 U_t + u_x &= 0 \\ \rho_3 u_t + \rho_4 U_t + U_x &= 0 \end{aligned} \tag{8}$$

this can be written in matrix form as

$$\mathbf{R}\mathbf{X}_t + \mathbf{X}_x = \mathbf{O} \tag{9}$$

To evaluate the 4 unknown coefficients ρ_i of (8), the positive roots of the characteristic equation and the eigenvector of (8) are to be established as equal to those of (3). From this condition, the four unknown coefficients may be determined

$$\rho_1 = (v_1\beta_1 - v_2\beta_2)/[v_1v_2(\beta_1 - \beta_2)], \qquad \rho_2 = (v_1 - v_2)/[v_1v_2(\beta_1 - \beta_2)]$$
$$\rho_3 = [\beta_1\beta_2(v_2 - v_1)]/[v_1v_2(\beta_1 - \beta_2)], \qquad \rho_4 = (v_2\beta_1 - v_1\beta_2)/[v_1v_2(\beta_1 - \beta_2)] \tag{10}$$

Since the constitutive relationship can be expressed as

$$\mathbf{S} = \mathbf{K}\mathbf{X}_x \tag{11}$$

where $\mathbf{S} = [\sigma'' - (\alpha - n)p, -np]^T$ is the vector of stresses for one-dimensional propagation, the following viscous-type boundary condition is obtained from (9)

$$\mathbf{S} = -\mathbf{K}\mathbf{R}\mathbf{X}_t \tag{12}$$

Through some manipulation, it can be demonstrated that the matrix **KR** is symmetric. The terms of this matrix are the values of the viscous dashpots, needed to ensure a transmitting boundary for both kinds of longitudinal wave of a two-phase medium, in which viscous coupling is small. It becomes apparent that viscous forces have to be related not only to absolute velocities but also to the relative velocities between the two phases, i.e., the matrix is not diagonal. From now on, the matrix **KR** could be written as

$$\mathbf{K}\mathbf{R} = \begin{bmatrix} c_{L1} & c_{L2} \\ c_{L2} & c_{L3} \end{bmatrix} \tag{13}$$

For $k = 0$, i.e., for a high viscous coupling typical of a low coefficient of permeability, as well as of low frequencies, and for null body forces ($b_1 = 0$), the equations of motion for one-dimensional propagation come down to:

$$\rho u_{tt} + cu_{xx} = 0$$
$$\rho U_{tt} + cU_{xx} = 0 \tag{14}$$

where

$$c = \lambda + 2\mu + \alpha^2 Q, \qquad \rho = (1 - n)\rho_s + n\rho_f \tag{15}$$

The system of partial differential equations, the solution of which enables waves to travel only in the positive x-direction, is still obtained by equation (8) with

$$\rho_1 = 1/v_{cl}, \qquad \rho_2 = 0$$
$$\rho_3 = 0, \qquad \rho_4 = 1/v_{cl} \tag{16}$$

where $v_{cl} = \sqrt{c/\rho}$ is the velocity of propagation with no relative motion between the solid and the fluid phases. In this case, viscous forces are only related to the absolute values of the velocities of the two phases. The silent boundary presented coincides with the classic viscous boundary for one-phase media: for high viscous coupling the saturated porous medium behaves like a one-phase medium.

The extension of the previous two kinds of silent boundary condition to u–w and u–p–U formulations is straightforward.

The first-order differential equation system (9) can easily be generalized in a higher-order differential operator, which can absorb plane waves propagating at angles of incidence $\mp\alpha_i$

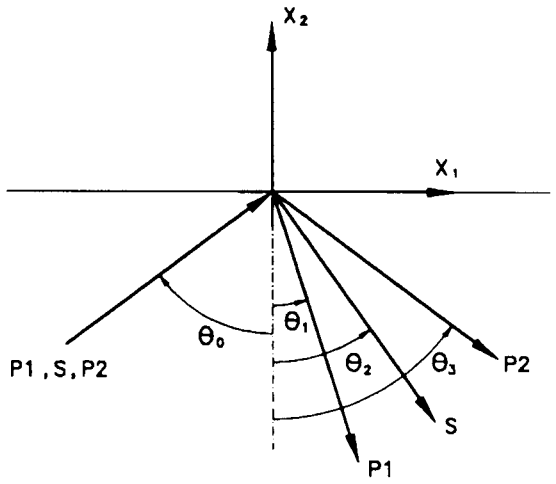

Figure 1. Incident and reflected waves

($i = 1, \ldots, n$), by using the method proposed by Higdom[18,19] for one-phase media. With regard to the second order, for the sake of simplicity, and considering only a rectilinear boundary as shown in Figure 1, the differential operator is

$$\left[\mathbf{R}^{-1}\frac{\partial}{\partial x_2} + \cos\alpha_p \frac{\partial}{\partial t}\right]\left[v_s \frac{\partial}{\partial x_2} + \cos\alpha_s \frac{\partial}{\partial t}\right] \tag{17}$$

where x_2 is the axis normal to the silent boundary and v_s is the rotational wave velocity

$$v_s = \sqrt{\frac{\mu}{(1-n)\rho_s + \dfrac{\rho_a}{\rho_f + \rho_a}\rho_f}} \tag{18}$$

if the viscous coupling is low. This operator can be applied to both displacement components at the silent boundary, i.e., u_2U_2 and u_1U_1, respectively. Here the angles α_p and α_s can be chosen to minimize spurious reflections by taking into account the geometric and dynamic properties of a given problem. The first factor in (17) yields perfect adsorption for P1- and P2-waves travelling at angles of incidence $\mp\alpha_p$, the second yields perfect absorption for S-waves travelling at angles of incidence $\mp\alpha_s$. Moreover, the first factor helps to absorb S-waves, while the second helps to absorb P1- and P2-waves. Finally, such an operator can be generalized for orders higher than two by using further terms in (17).

4. WAVE REFLECTION ANALYSIS

For the sake of simplicity, the assessment of the theoretical performance of the proposed silent boundary method is done in relation to the first-order method in a porous medium in which the permeability, or the frequency of the driving pulse, is high. A plane harmonic elastic wave is assumed to impinge upon a rectilinear boundary, as shown in Figure 1. The analysis is similar to the one by Cohen and Jennings[12] for a silent boundary in a one-phase medium. The same notation generally used for analysing wave reflections at the free surface of one-phase media (see References 43 for instance) is used here. The following analysis gives the same results as were

obtained by Deresiewicz[44] for the reflection of plane harmonic waves at a free surface of a saturated porous medium, if the silent boundary is eliminated. Both the incident and the reflected waves can then be written as

$$u_i^{(m)} = A_m d_i^{(m)} \exp(\mathrm{i}\eta_m)$$
$$U_i^{(m)} = \beta_j A_m d_i^{(m)} \exp(\mathrm{i}\eta_m) \tag{19}$$

where different values of the index m label the various types of waves, β_j is equal to β_1 and β_2 for longitudinal waves of the first and second kind, respectively, and is equal to β_s, for the rotational wave, with

$$\beta_s = -\frac{\rho_{12}}{\rho_{22}} \tag{20}$$

and

$$\eta_m = k_m(x_1 p_1^{(m)} + x_2 p_2^{(m)} - v_m t). \tag{21}$$

The unit propagation vectors, $\mathbf{d}^{(m)}$ and $\mathbf{p}^{(m)}$, have components $d_i^{(m)}$ and $p_i^{(m)}$ and are the same as those used for analysing the wave reflection at a free surface in one-phase media (see References 43 for instance). The velocity v_m is equal to v_1 and v_2 for longitudinal waves of the first and second kind, respectively, and is equal to v_s for the rotational wave [equation (18)]. The index m takes on the value $m = 0$ for the incident wave, which may be either a longitudinal wave of the first kind (P1-wave) or a rotational wave (S-wave) or a longitudinal wave of the second kind (P2-wave). For the reflected waves the index m takes on the following values: $m = 1$ for the reflected P1-wave, $m = 2$ for the reflected S-wave and $m = 3$ for the reflected P2-wave.

The displacements and the stresses at the boundary ($x_2 = 0$) are obtained by replacing the term η_m by $\bar{\eta}_m$, where

$$\bar{\eta}_m = k_m(x_1 p_1^{(m)} - c_m t). \tag{22}$$

In $x_2 = 0$ the relevant stresses are σ''_{22}, σ''_{21} and p, which may be calculated from equation (2) as follows

$$\begin{aligned}
\sigma''^{(m)}_{22} - (\alpha - n)p^{(m)} &= \mathrm{i}k_m\{[\lambda + 2\mu + (\alpha - n)^2 Q]\, d_2^{(m)} p_2^{(m)} + (\lambda + (\alpha - n)^2 Q)\, d_1^{(m)} p_1^{(m)}\} A_n \exp(\mathrm{i}\bar{\eta}_m) \\
&\quad + \mathrm{i}k_m n(\alpha - n)Q[d_2^{(m)} p_2^{(m)} + d_1^{(m)} p_1^{(m)}]\, \beta_m A_m \exp(\mathrm{i}\bar{\eta}_m) \\
\sigma''^{(m)}_{21} &= \mathrm{i}k_m \mu[d_2^{(m)} p_1^{(m)} + d_1^{(m)} p_2^{(m)}] A_m \exp(\mathrm{i}\bar{\eta}_m) \\
-np^{(m)} &= \mathrm{i}k_m n(\alpha - n)Q[d_2^{(m)} p_2^{(m)} + d_1^{(m)} p_1^{(m)}] A_m \exp(\mathrm{i}\bar{\eta}_m) \\
&\quad + \mathrm{i}k_m n^2 Q[d_2^{(m)} p_2^{(m)} + d_1^{(m)} p_1^{(m)}]\, \beta_m A_m \exp(\mathrm{i}\bar{\eta}_m).
\end{aligned} \tag{23}$$

At the boundary, the stresses are set as equal to the viscous stresses generated by the proposed method.

$$\sigma''_{22} - (\alpha - n)p = \sum_{m=1}^{4} [\sigma''^{(m)}_{22} - (\alpha - n)p^{(m)}] = -c_{L1} \sum_{m=1}^{4} \dot{u}_2^{(m)} - c_{L2} \sum_{m=1}^{4} \dot{U}_2^{(m)}$$

$$\sigma''_{21} = \sum_{m=1}^{4} \sigma''^{(m)}_{21} = -c_{S1} \sum_{m=1}^{4} \dot{\mu}_1^{(m)} \tag{24}$$

$$-np = n \sum_{m=1}^{4} p^{(m)} = -c_{L2} \sum_{m=1}^{4} \dot{u}_2^{(m)} - c_{L3} \sum_{m=1}^{4} \dot{U}_2^{(m)} \tag{25}$$

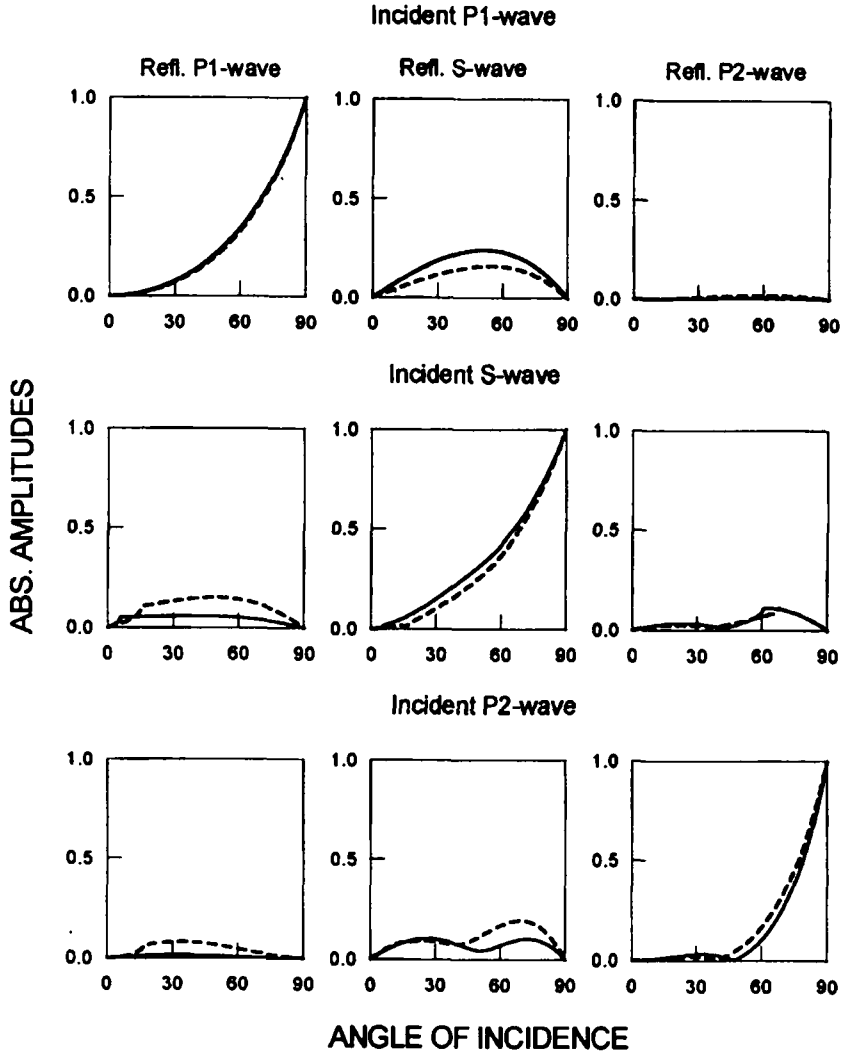

Figure 2. Absolute amplitudes of reflected waves for various angles of incidence (plain strain problem) for $\lambda = 0{\cdot}865 \times 10^9$ dyn/cm^2 and $\mu = 0{\cdot}577 \times 10^9$ dyn/cm^2 (——) and for $\lambda = 0{\cdot}692 \times 10^{10}$ dyn/cm^2 and $\mu = 0{\cdot}461 \times 10^{10}$ dyn/cm^2 (- - - -)

where c_{S1} is the value of viscous dashpots for rotational waves (see Appendix II). Observations of $\bar{\eta}_m$ reveals the relationships among k_m, θ_m and v_m given in Appendix I.

The solution to the three systems of three equations is shown graphically in Figure 2 for two porous media with different stiffness characteristics: they correspond, respectively, to a cohesionless soil at low confining pressures ($\lambda = 0{\cdot}865 \times 10^9$ dyn/cm^2 and $\mu = 0{\cdot}577 \times 10^9$ dyn/cm^2), and at very high confining pressures ($\lambda = 0{\cdot}692 \times 10^{10}$ dyn/cm^2 and $\mu = 0{\cdot}461 \times 10^{10}$ dyn/cm^2). For both materials, the remaining material properties are

$$K_s = 0{\cdot}3600 \times 10^{12} \text{ dyn/cm}^2 \qquad n = 0{\cdot}40 \qquad K_f = 0{\cdot}2177 \times 10^{11} \text{ dyn/cm}^2$$

$$\rho_f = 1 \text{ g/cm}^3 \qquad \rho_s = 2{\cdot}70 \text{ g/cm}^3 \qquad \rho_a = 0 \text{ g/cm}^3. \tag{25}$$

By comparing Figure 2 with the corresponding results obtained by Cohen and Jennings[12] for one-phase media, it becomes apparent that the overall behaviour of the proposed method for two-phase media is similar to the behaviour of the viscous boundary for one-phase media, providing the ratio between the rotational and longitudinal wave velocities v_s/v_p is equal in the two media. It should be noted that for incident S-waves and P2-waves, when the incidence angle is greater than a critical value, reflected P1- and P2-waves and P1- and S-waves, respectively, may become surface waves which travel along the boundary. The critical angles may be detected in Figure 2 in line with the abrupt changes in slope. Such surface waves are confined to a region near the boundary, in fact their amplitudes exponentially decrease with depth and contain only a small fraction of the total energy. The fact that their superficial amplitude might be large is therefore not severely detrimental.

The efficiency of the silent boundary developed for low viscous coupling when it is applied to high viscous coupling is not shown because the results are practically indistinguishable from those for low viscous coupling (Figure 2). In fact, the greater the solid skeleton stiffness, the closer the efficiency between high and low viscous coupling media: the ratio v_1/v_{c1} tends towards unity as the stiffness of the solid skeleton increases.

5. FINITE ELEMENT SOLUTION

After semidiscretization by the usual finite element technique,[45] the differential dynamic equilibrium equations give rise to the following symmetrical system of equations:[35,39]

$$\begin{bmatrix} \mathbf{M}_s & -\mathbf{M}_a \\ -\mathbf{M}_a^T & \mathbf{M}_f \end{bmatrix} \begin{bmatrix} \ddot{\mathbf{u}} \\ \ddot{\mathbf{U}} \end{bmatrix} + \begin{bmatrix} \mathbf{C}_1 & \mathbf{C}_2 \\ \mathbf{C}_2^T & \mathbf{C}_3 \end{bmatrix} \begin{bmatrix} \dot{\mathbf{u}} \\ \dot{\mathbf{U}} \end{bmatrix} + \begin{bmatrix} \mathbf{K} & \mathbf{G}_1 \\ \mathbf{G}_1^T & \mathbf{P} \end{bmatrix} \begin{bmatrix} \mathbf{u} \\ \mathbf{U} \end{bmatrix} = \begin{bmatrix} \mathbf{f}_s \\ \mathbf{f}_f \end{bmatrix} \tag{26}$$

where $\mathbf{u}$ and $\mathbf{U}$ are the unknown nodal values. The silent boundary condition comes down to the calculation of the following damping matrix for each boundary element:

$$\begin{bmatrix} \mathbf{C}_{B1} & \mathbf{C}_{B2} \\ \mathbf{C}_{B2} & \mathbf{C}_{B3} \end{bmatrix} \tag{27}$$

where the matrices $\mathbf{C}_{Bi}$ are given in Appendix II. The matrices $\mathbf{C}_{B1}$, $\mathbf{C}_{B2}$ and $\mathbf{C}_{B3}$ have to be assembled into the global damping matrix.

The time integration of the coupled differential system (26) is solved by using Newmark's algorithm.[46-47]

6. NUMERICAL RESULTS

Three numerical examples are produced in order to show the accuracy and reliability of the above-described method for generating silent boundary conditions. Both one-dimensional and two-dimensional (axisymmetric and plane strain) propagation is analysed.

First, some one-dimensional results are shown to demonstrate the reliability of the silent boundary condition obtained for the extreme values of viscous coupling, for problems where the value of permeability is finite (test problem 1).

Thereafter, the accuracy of the silent boundary condition is examined for waves striking the boundary at angles of incidence other than zero. In fact, judging from the theoretical analysis developed in Section 4, this method is expected to produce spurious reflected waves, the amplitude of which increases with the angle of incidence. A two-dimensional plane strain propagation problem is consequently solved, in order to analyse the behaviour of this kind of silent boundary condition with a plane wave striking at an angle of incidence of 50° (test problem 2).

Finally, the application of such a method to a practical problem is illustrated. With reference to non-destructive dynamic pile tests, the axisymmetric propagation of elastic waves along a pile shaft is evaluated (test problem 3).

Since spatial and temporal refinements are linked, the time steps in all the following examples are chosen a little smaller than the time interval needed for the fastest wave to propagate between two adjacent nodes.

6.1. Test problem 1

This is an analysis of the behaviour of the proposed boundary condition for perpendicular incident longitudinal waves. Rotational waves are not analysed in detail because their behaviour may be easily deduced from the behaviour of the longitudinal waves of the first kind. This analysis is carried out using one-dimensional finite elements. The solid skeleton stiffness is given by $\lambda = 0{\cdot}692 \times 10^{10}$ dyn/cm^2 and $\mu = 0{\cdot}461 \times 10^{10}$ dyn/cm^2, whereas the remaining material properties are the same as those considered in Section 4 at (25). Three values of permeability are considered: one very large ($k = 1 \times 10^{-1}$ cm^3 s/g), one very small ($k = 1 \times 10^{-9}$ cm^3 s/g), and one intermediate ($k = 1 \times 10^{-4}$ cm^3 s/g, in order to show the behavior of the silent boundary conditions developed for high and low viscous coupling. A finite soil column 10 cm in length is considered. The excitation applied at the top surface consists of a step velocity boundary condition to both solid and fluid phases.

The spatial discretization involves 50 one-dimensional quadratic finite elements. The temporal integration involves 440 steps of 0·5 μs, for a total period of 220 μs, during which 2 reflections of the longitudinal wave of the first kind and 1 reflection of the longitudinal wave of the second kind are allowed.

Figures 3–6 show the numerical results relative to the silent boundary condition for $k = \infty$ and for $k = 0$, respectively. Only longitudinal waves are represented, since similar results are obtained for rotational waves.

Figures 3 and 4 show that the use, for instance, of the silent boundary condition for very previous materials ($k = \infty$) with an impervious material ($k = 1 \times 10^{-9}$ cm^3 s/g), gives a spurious reflected wave with an amplitude of about 1 per cent of the amplitude of the incident wave, which is consistent with theoretical predictions obtainable from the relationships in Section 4.

Figures 5 and 6 show that the silent boundary condition for $k = 0$ generally gives greater spurious reflections than the silent boundary condition for $k = \infty$, and it behaves well only for high viscous coupling or low-frequency pulses or for considerable travel lengths, when higher frequency components are practically damped out and the porous medium behaves as a one-phase medium. In the case of the intermediate permeability shown in Figures 5 and 6 ($k = 1 \times 10^{-4}$ cm^3 s/g), the silent boundary conditions for $k = \infty$ behave much better, because for this permeability value the incident wave near the boundary is still travelling at a velocity similar to that of null viscous coupling, and the wave of the second kind is not damped out.

For practical applications, once the frequency content of the transient pulse, the permeability value and the travel length are known, it is easy to select which kind of silent boundary condition is the most suitable.[41]

6.2. Test problem 2

The plain strain problem shown in Figure 7 is solved. At the top surface of the two-dimensional domain, an effective load of 1 MPa, varying as a single sine of a period of 100 μs, is applied to the solid skeleton only. The material properties are the same as those in the previous test problem,

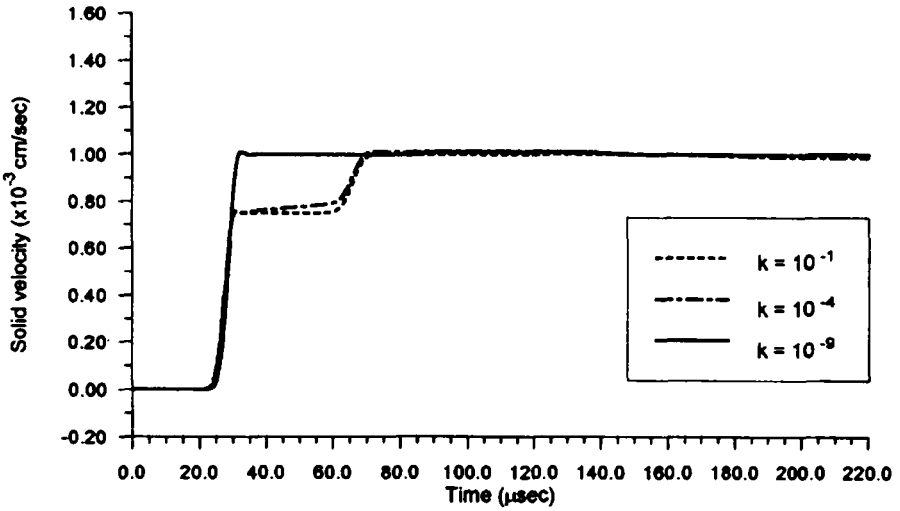

Figure 3. Solid skeleton velocity history at 5 cm, for the silent boundary condition $k = \infty$: *for* $k = 1 \times 10^{-1}$ cm^3 s/g, $k = 1 \times 10^{-4}$ cm^3 s/g and $k = 1 \times 10^{-9}$ cm^3 s/g

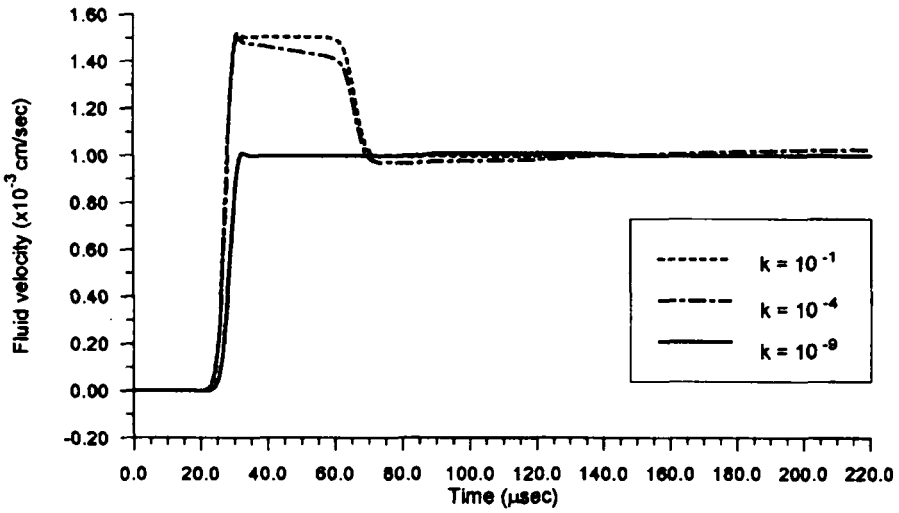

Figure 4. Fluid skeleton velocity history at 5 cm, for the silent boundary condition $k = \infty$: *for* $k = 1 \times 10^{-1}$ cm^3 s/g, $k = 1 \times 10^{-4}$ cm^3 s/g and $k = 1 \times 10^{-9}$ cm^3 s/g

with $k = 1 \times 10^{-3}$ cm^3 s/g. The spatial discretization involves 265 two-dimensional quadratic finite elements, with sizes of about 1×1 cm^2. The time integration involves 440 steps of 2.0 μs, for a total period of 880 μs.

Figure 8 shows the distribution of the vertical displacements of the solid skeleton, at three different times. The partially reflected wave of the first kind is seen to have an amplitude of about 10% of the initial amplitude, whereas the partially reflected wave of the second kind has an amplitude of only 2–3% of the amplitude of the incident wave of the second kind. This is consistent with the theoretical predictions of Figure 2.

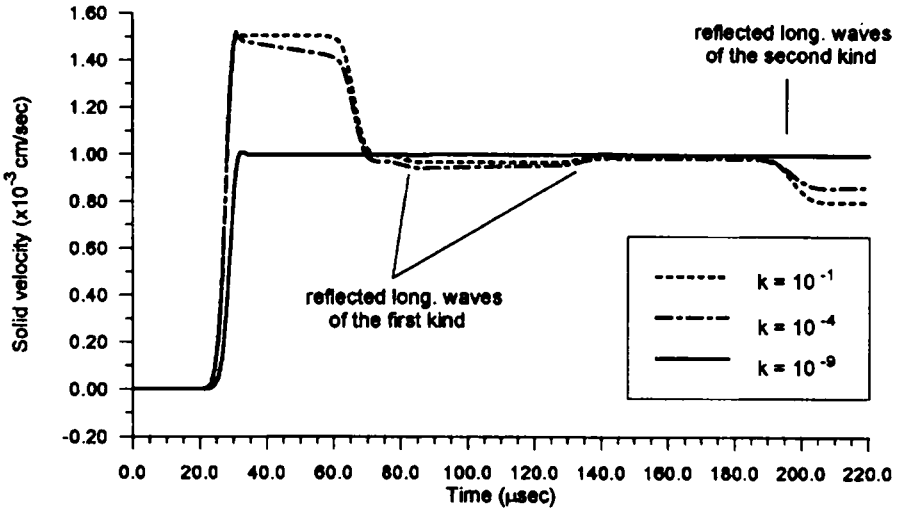

Figure 5. Solid skeleton velocity history at 5 cm, for the silent boundary condition $k = 0$: *for* $k = 1 \times 10^{-1}$ cm^3 s/g, $k = 1 \times 10^{-4}$ cm^3 s/g and $k = 1 \times 10^{-9}$ cm^3 s/g

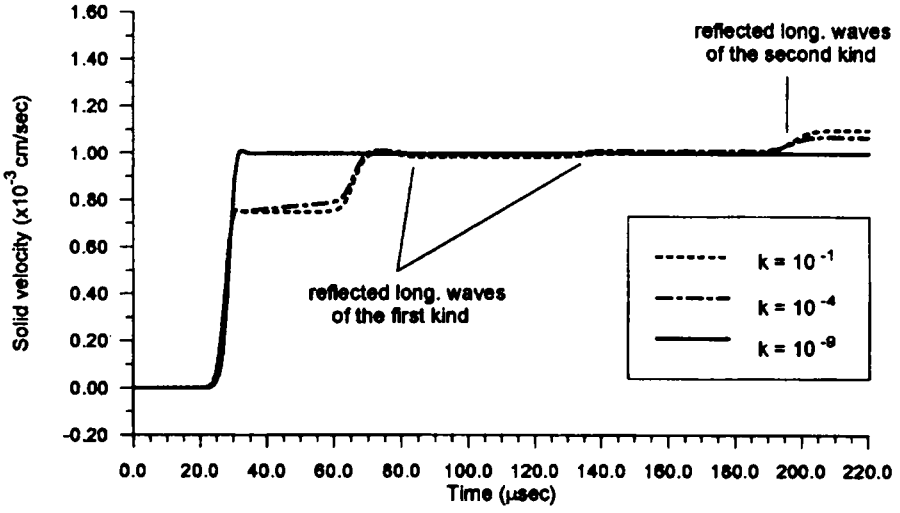

Figure 6. Fluid skeleton velocity history at 5 cm, for the silent boundary condition $k = 0$: *for* $k = 1 \times 10^{-1}$ cm^3 s/g, $k = 1 \times 10^{-4}$ cm^3 s/g and $k = 1 \times 10^{-9}$ cm^3 s/g

6.3. Test problem 3

The propagation of a longitudinal wave travelling along a pile shaft is analysed to verify the reliability of the proposed boundary condition for a practical engineering problem. Figure 9 shows the geometry of the pile. The material properties are as follows.

— for the concrete pile: $\lambda = 1{\cdot}154 \times 10^{11}$ dyn/cm^2, $\mu = 0{\cdot}769 \times 10^{11}$ dyn/cm^2 and $k = 1 \times 10^{-8}$ cm^3 s/g;

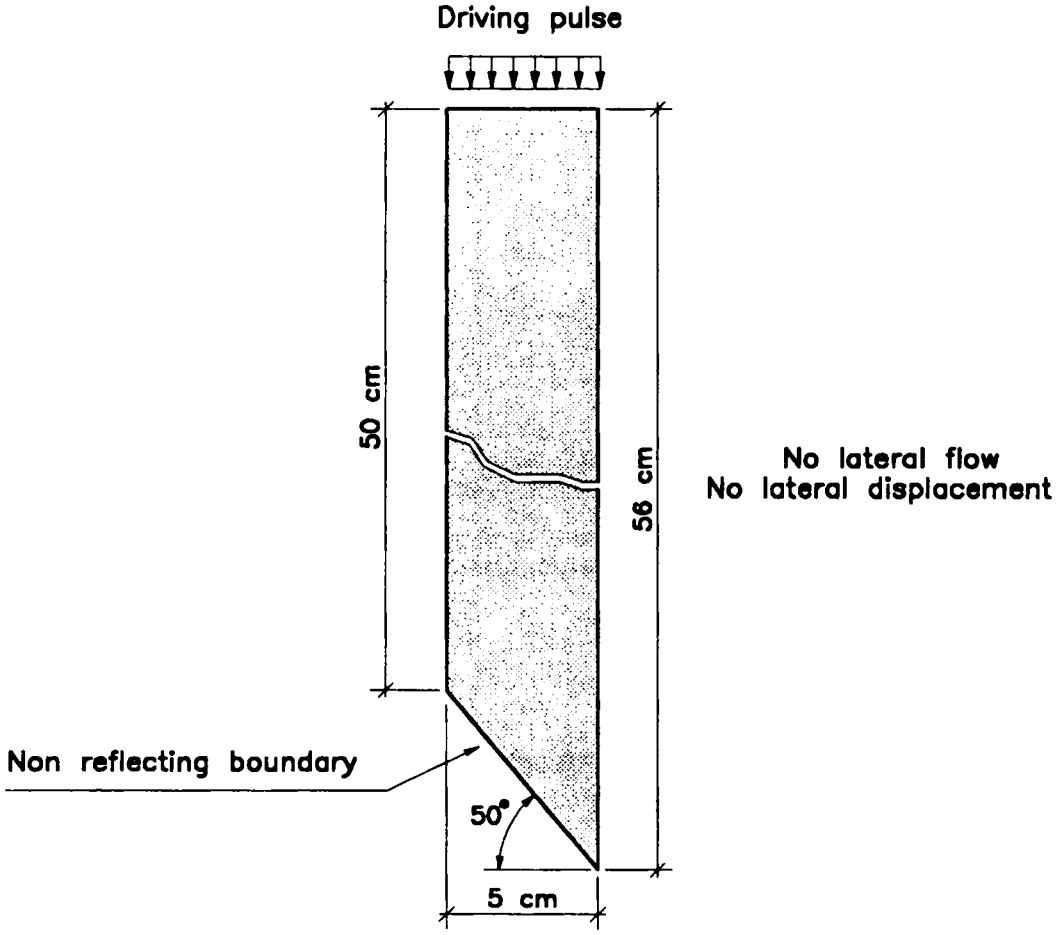

Figure 7. Geometry of the plain strain problem (test problem 2)

— for the soil: $\lambda = 0{\cdot}692 \times 10^{10}$ dyn/cm^2, $\mu = 0{\cdot}461 \times 10^{10}$ dyn/cm^2 and $k = 1 \times 10^{-5}$ cm^3 s/g; the remaining material properties are the same of those considered in Section 4 at (25).

The spatial discretization involves 40 two-dimensional quadratic finite elements (with a size of about $0{\cdot}50 \times 0{\cdot}25$ m^2) for the pile and 154 quadratic finite elements (with a size ranging from about $0{\cdot}60 \times 0{\cdot}25$ m^2 to $0{\cdot}30 \times 0{\cdot}25$ m^2) for the soil. The temporal integration involves 250 steps of 50 μs, for a total period of 12 500 μs.

The driving pulse is given by a vertical velocity boundary condition applied to both solid and fluid phases at the top surface of the pile. The driving pulse varies in amplitude with a single cosine wave with a period of 2500 μs (400 Hz), with an offset equal to the amplitude.

In Figure 10, the distribution of the solid skeleton's vertical velocities is shown at three different times. The silent boundary condition is clearly quite effective in eliminating unwanted reflections. The fast propagation of a longitudinal wave along the pile shaft is accompanied by a short rotational wave in the soil. Since a wave is only adequately represented if the element sizes are smaller than the wavelength, a large number of small elements is needed for the spatial discretizations of the soil. Figure 10 shows that this boundary condition allows a reduction in the

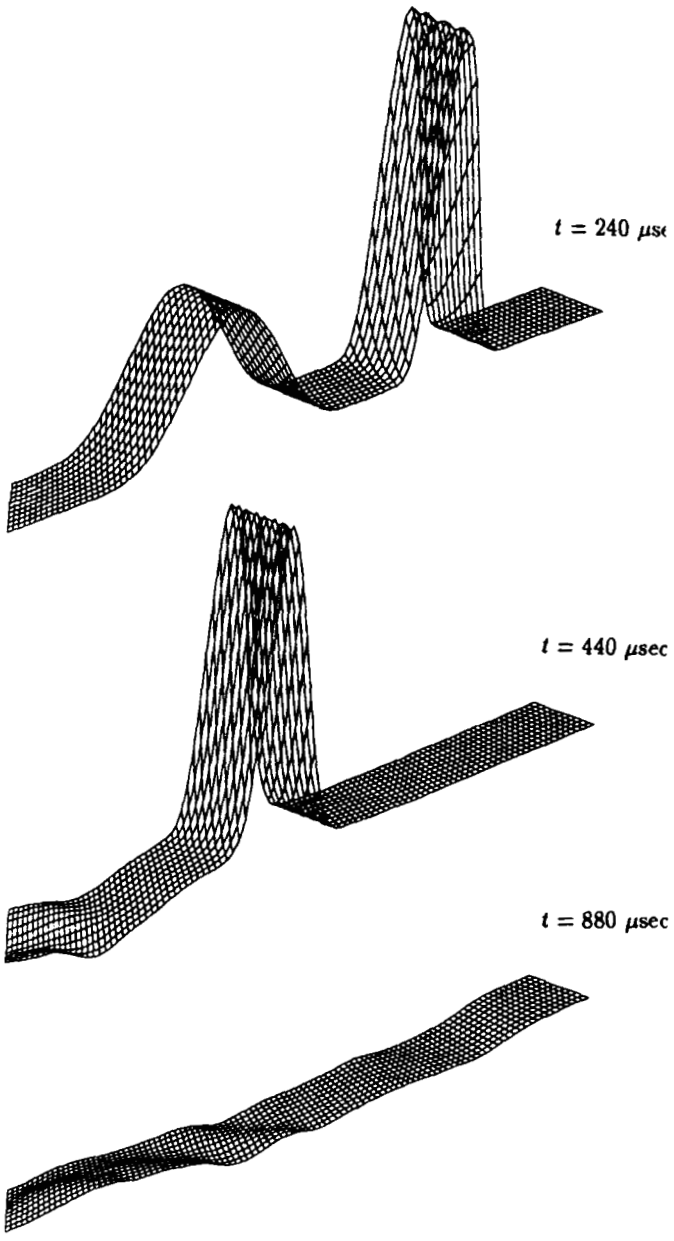

Figure 8. Distribution of vertical solid skeleton displacements, for the silent boundary condition $k = \infty$: *in* $t = 240$ μs, in $t = 440$ μs and in $t = 880$ μs

computational grid representing the soil and consequently also allows a reduction in the size of finite elements representing the soil, for the purpose of achieving a greater accuracy.

Figures 11 and 12 show the history of vertical and horizontal solid skeleton velocities, of a point placed on the surface of the shaft half way up the pile. The results obtained with a much smaller computational grid are also shown for comparison. The second computational grid is

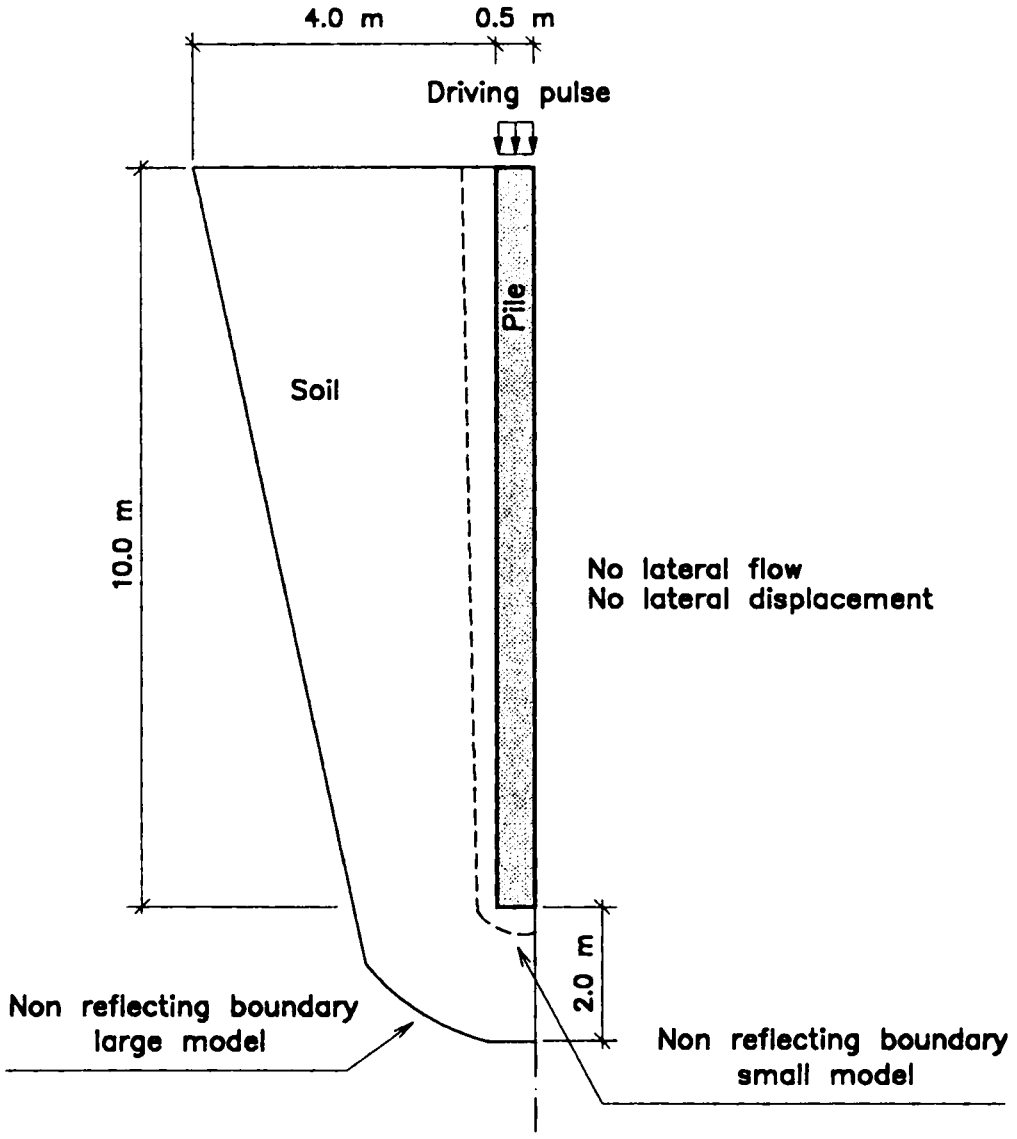

Figure 9. Geometry of the axisymmetric problem, regarding the propagation of a longitudinal wave along a pile shaft (test problem 3)

formed of the same number of elements for the pile (40 elements), but only the first layer of soil elements in contact with the pile (22 elements). The results obtained with the two meshes is highly consistent, especially for the main pulse, while some differences exist among the reflected pulses at the pile base, because of the presence of spurious reflections of low amplitude from the silent boundaries.

It should be added that this silent boundary was found to give greater spurious reflections in axisymmetric problems than in plane strain problems; in fact the effectiveness of this method in axisymmetric problems may be demonstrated to be dependent on the frequency of the impinging wave, as in the case of the viscous boundary for one-phase media.[12]

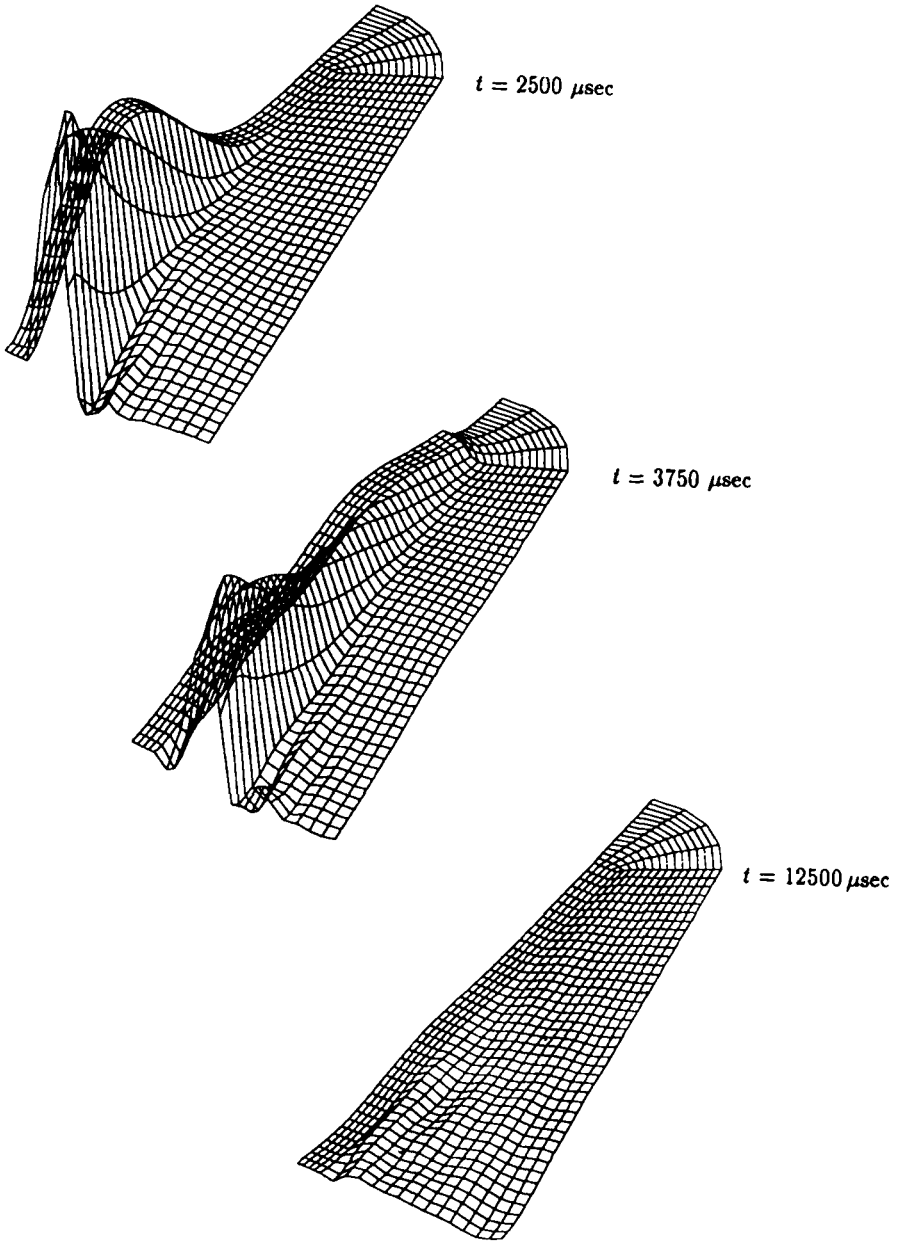

Figure 10. Distribution of vertical solid skeleton velocities, for the silent boundary conditions $k = \infty$: *in* $t = 2500\ \mu s$, in $t = 3750\ \mu s$ and in $t = 12\,500\ \mu s$

7. CONCLUDING REMARKS

This work presents an easy silent boundary implementation, for the transient analysis of wave propagation problems in porous saturated elastic media. The non-reflecting condition is developed as an extension to the multidirectional boundary for two-phase media, by satisfying the

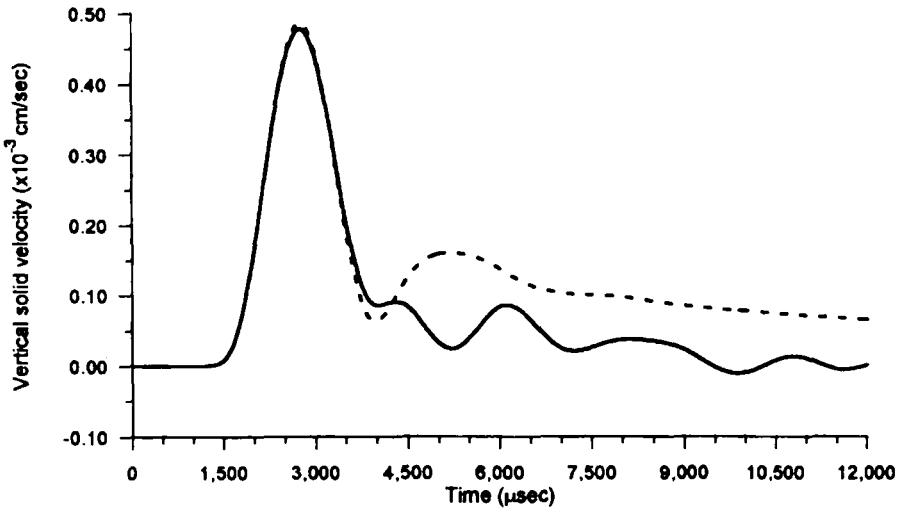

Figure 11. Vertical solid skeleton velocity history at $z = 5{\cdot}00$ m, for the silent boundary condition $k = \infty$: (——) large mesh of 154 finite elements for the soil, (- - -) small mesh of 22 finite elements for the soil

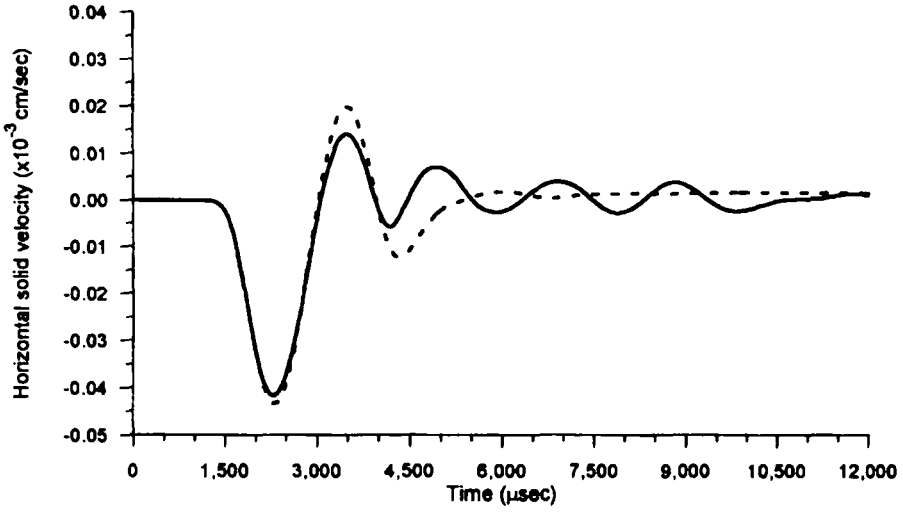

Figure 12. Horizontal solid skeleton velocity history at $z = 5{\cdot}00$ m, for the silent boundary condition $k = \infty$: (——) large mesh of 154 finite elements for the soil, (- - -) small mesh of 22 finite elements for the soil

condition of waves travelling only in a single direction. Only the extreme values of viscous coupling (i.e., null and infinite) must be considered in the derivation of the boundary conditions, since for intermediate viscous coupling, the error made using the solution for $k = \infty$ is limited to 1% at the most.

The effectiveness of the proposed method is theoretically analysed for the first-order boundary. The results given in Sections 4 and 6 show the reliability of the method in avoiding, or at least significantly reducing, the unwanted reflections of waves in 1D and 2D unbounded two-phase

problems, for angles of incidence both equal to and greater than zero. Therefore, in soil–structure interaction problems, the boundary condition presented enables a substantial decrease in the representative size of the domain surrounding the structure (i.e., the soil surrounding the pile shaft in the third test problem), and in the resulting computational effort of the numerical analysis.

The advantage of the silent boundary presented here is its independence of the frequency of the outgoing wave (for one-dimensional and plane strain problems). Moreover, the first-order boundary can easily be implemented and has low computational costs, since it requires only the calculation of a viscous-type matrix for each boundary element.

A comparison of the efficiency of the first-order boundary presented here with the higher-order multidirectional boundaries shown in Section 4 will be the subject of a future paper.

APPENDIX I

The inspection of $\bar{\eta}_m$ leads to some relationships among k_m, θ_m and v_m. For instance, for an incident P1-wave, the relationships are as follows:

$$\begin{gathered} \kappa_1 = v_1/v_s, \qquad \kappa_2 = v_1/v_2 \\ k_1 = k_0, \qquad k_2 = \kappa_1 k_0, \qquad k_3 = \kappa_2 k_0 \\ \theta_1 = \theta_0, \qquad \sin\theta_2 = \sin\theta_0/\kappa_1, \qquad \sin\theta_3 = \sin\theta_0/\kappa_2 \end{gathered} \tag{28}$$

The corresponding relationships for an incident S-wave and P2-wave can be obtained in the same way. It should be noted that for incident S- and P2-waves, some θ_i may be complex. This means that the corresponding reflected waves are surface waves.

APPENDIX II

The matrices $\mathbf{C}_{Bi}$ are, respectively, defined by

$$\begin{aligned} \mathbf{C}_{B1} &= \int_\Gamma \mathbf{N}^{u\mathrm{T}} \mathbf{t} \mathbf{C}_{b1} \mathbf{t}^{\mathrm{T}} \mathbf{N}^{u} \, \mathrm{d}\Gamma \\ \mathbf{C}_{B2} &= \int_\Gamma \mathbf{N}^{u\mathrm{T}} \mathbf{t} \mathbf{C}_{b2} \mathbf{t}^{\mathrm{T}} \mathbf{N}^{U} \, \mathrm{d}\Gamma \\ \mathbf{C}_{B3} &= \int_\Gamma \mathbf{N}^{U\mathrm{T}} \mathbf{t} \mathbf{C}_{b3} \mathbf{t}^{\mathrm{T}} \mathbf{N}^{U} \, \mathrm{d}\Gamma \end{aligned} \tag{29}$$

where

$$\begin{aligned} \mathbf{C}_{b1} &= \begin{bmatrix} c_{L1} & 0 \\ 0 & c_{S1} \end{bmatrix} \\ \mathbf{C}_{b2} &= \begin{bmatrix} c_{L2} & 0 \\ 0 & 0 \end{bmatrix} \\ \mathbf{C}_{b3} &= \begin{bmatrix} c_{L3} & 0 \\ 0 & 0 \end{bmatrix} \end{aligned} \tag{30}$$

and

$$t = \begin{bmatrix} \cos(\alpha) & -\sin(\alpha) \\ \sin(\alpha) & \cos(\alpha) \end{bmatrix} \tag{31}$$

with α being the angle between the normal to the boundary and the positive x-axis, and c_{S1} the value of viscous dashpots for rotational waves:

$$c_{S1} = \sqrt{G((1-n)\rho_s + n\rho_f\rho_a/(n\rho_f + \rho_a))} \quad \text{for } k = \infty$$
$$c_{S1} = \sqrt{G((1-n)\rho_s + n\rho_f)} \quad \text{for } k = 0 \tag{32}$$

REFERENCES

1. D. Givoli, 'Non-reflecting boundary conditons: a review', *J. Comput. Phys.* **94,** 1–29 (1991)
2. O. C. Zienkiewicz, D. W. Kelly and P. Bettess, 'The coupling of the finite element method and boundary solution procedure', *Int. j. numer. methods eng.*, **11,** 355–375 (1977).
3. H. L. Wong, 'Effect of surface topology on the diffraction of P, SV and Rayleigh waves', *Bull. Seism. Soc. Am.*, **72,** 1167–1183 (1982).
4. F. J. Sanchez-Sesma, 'Diffraction of elastic waves by three-dimensional surface irregularities', *Bull. Seism. Soc. Am.*, **73,** 1621–1636 (1983).
5. K. R. Khair, S. K. Datta and A. H. Shah, 'Amplification of obliquely incident seismic waves by cylindrical alluvial valleys of arbitrary cross-sectional shapes, Part I: Incident P and SV waves', *Bull. Seism. Soc. Am.*, **79,** 610–630 (1989).
6. E. Kausel, 'Local transmitting boundaries', *J. Eng. Mech. Div ASCE*, **114,** 1011–1027 (1988).
7. H. Kawase, 'Time-domain response of a semi-circular canyon for incident SV, P and Rayleigh waves calculated by the discrete wave number boundary element method', *Bull. Seism. Soc. Am.*, **78,** 1415–1437 (1988).
8. D. Givoli, 'A numerical solution procedure for exterior wave problems', *Comput. Struct.*, **43,** 77–85 (1992).
9. J. Lysmer and R. L. Kuhlemeyer, 'Finite dynamic model for infinite media', *J. Eng. Mech. Div. ASCE*, **95,** 859–877 (1969).
10. W. White, S. Valliappan and I. K. Lee, 'Unified boundary for finite dynamic models', *J. Eng. Mech. Div. ASCE*, **103,** 949–964 (1977).
11. A. Castellani, 'Boundary conditions to simulate an infinite space', *Meccanica*, **9,** 199–205 (1974).
12. M. Cohen and P. C. Jennings, 'Silent boundary methods for transient analysis', in T. Belytschko and T. J. R. Huges (eds), *Computational Methods for Transient Analysis*, Elsevier, Amsterdam, 1983, pp. 302–360.
13. R. Clayton and B. Enquist, 'Absorbing boundary conditions for acoustic and elastic wave equations', *Bull. Seism. Soc. Am.*, **67,** 1529–1540 (1977).
14. B. Engquist and A. Majda, 'Absorbing boundary conditions for the numerical simulation of waves', *Math. Comput.* **31,** 629–651 (1977).
15. T. J. R. Hughes, 'A simple scheme for developing upwind finite elements', *Int. j. numer. methods eng.*, **12,** 1359–1369 (1978).
16. K. D. Mahrer, 'An empirical study of instability and improvement of absorbing boundary conditions for the elastic wave equation', *Geophys*, **51,** 1499–1501 (1986).
17. E. Kausel, 'Physical interpretation and stability of paraxial boundary conditions', *Bull. Seism. Soc. Am.*, **82,** 898–913 (1992).
18. R. L. Higdom, 'Radiation boundary conditions for elastic wave propagation', *SIAM J. Numer. Anal.*, **27,** 831–870 (1990).
19. R. L. Higdom, 'Absorbing boundary conditions for acoustic and elastic waves in stratified media', *J. Comput. Phys.*, **101,** 386–418 (1992).
20. Z. P. Liao and H. L. Wong, 'A transmitting boundary for the numerical simulation of elastic wave propagation', *Soil Dyn. Earthquake Eng.*, **3,** 133–144 (1984).
21. R. L. Higdom, 'Initial-boundary value problems for linear hyperbolic systems', *SIAM Rev.*, **28,** 177 217 (1986).
22. Z. P. Liao and J. B. Liu, 'Numerical instabilities of a local transmitting boundary', *Earthquake Eng. Struct. Dyn.*, **21,** 65–77 (1992).
23. C. Peng and M. N. Toksoz, 'An optimal absorbing boundary condition for finite difference modelling of acoustic and elastic wave propagation', *J. Acoust. Soc. Am.*, **95,** 733–745 (1994).
24. W. D. Smith, 'A non-reflecting plane boundary for wave propagation problems', *J. Comput. Phys.*, **15,** 492–503 (1974).
25. P. A. Cundall, 'Solution of infinite dynamic problems by finite modelling in time domain', *Proc. 2nd Int. Conf. Appl. Math. Modeling*, Madrid. 1978.
26. P. Bettess and O. C. Zienkiewicz, 'Diffusion and refraction of surface waves using finite and infinite elements', *Int. j. numer. methods eng.*, **11,** 1271–1290 (1977).

27. O. C. Zienkiewicz, K. Bando, P. Bettess, C. Emson and T. C. Chiam, 'Mapped infinite elements for exterior wave problems', *Int. j. numer. methods eng.*, **21**, 1229–1251 (1985).
28. Y. K. Chow and I. M. Smith, 'Static and periodic infinite elements', *Int. j. numer. methods eng.*, **17**, 503–526 (1981).
29. G. Degrande and G. De Roeck, 'An absorbing boundary condition for wave propagation in saturated poroelastic media. Part I: Formulation and efficiency evalution', *Soil Dyn. Earthquake Eng.*, **12**, 411–421 (1993).
30. G. Degrande and G. De Roeck, 'An absorbing boundary condition for wave propagation in saturated poroelastic media. Part II: Finite element formulation', *Soil Dyn. Earthquake Eng.*, **12**, 423–432 (1993).
31. M. A. Biot, 'General theory of three-dimensional consolidation', *J. Appl. Phys.*, **12**, 155–164 (1941).
32. M. A. Biot, 'Theory of propagation of elastic waves in a fluid saturated porous solid', *J. Acoust. Soc. Am.*, **38**, 168–191 (1956).
33. M. A. Biot, 'Mechanics of deformation and acoustic propagation in porous media', *J. Appl. Phys.*, **33**, 1482–1498 (1962).
34. M. A. Biot, 'Generalized theory of acoustic propagation in porous dissipation media', *J. Acoust. Soc. Am.*, **34**, 1254–1264 (1962).
35. A. H. D. Cheng, T. Badmus and D. E. Beskos, 'Integral equation for dynamic poroelasticity in frequency domain with BEM solution', *J. Eng. Mech. Div. ASCE*, **117**, 1136–1157 (1991).
36. J. Chen, 'Time domain fundamental solution to Biot's complete equations of dynamic poroelasticity. Part I: two-dimensional solution', *Int. J. Solids Struct.*, **31**, 1447–1490 (1994).
37. O. C. Zienkiewicz and T. Shiomi, 'Dynamic behaviour of saturated porous media: the generalized Biot formulatlion and its numerical solution', *Int. J. Numer. Anal. Methods Geomech.*, **8**, 71–86 (1984).
38. B. R. Simon, J. S.-S. Wu, O. C. Zienkiewicz and D. K. Paul, 'Evaluation of u–w and u–π finite element methods for the dynamic response of saturated porous media using one-dimensional models', *Int. J. numer. Anal. Methods Geomech.*, **10**, 461–482 (1986).
39. A. Gajo, A. Saetta and R. Vitaliani, 'Evaluation of three and two field finite element methods for the dynamic response of saturated soil', *Int. j. numer. methods eng.*, **37**, 1231–1247 (1994).
40. S. K. Garg, H. Nayfeh and A. J. Good, 'Compressional waves in fluid-saturated elastic porous media', *J. Appl. Phys.*, **45**, 1968–1974 (1974).
41. A. Gajo, 'The influence of viscous coupling in the propagation of elastic waves in saturated soil', *J. Geotech. Eng. ASCE*, **121**, (9), 636–644 (1995).
42. A. Gajo and L. Mongiovi, 'An analytical solution for the transient response of saturated porous elastic solids', *Int. J. Numer. Anal. Methods Geomech.*, **19**, 399–414 (1995).
43. J. D. Achenbach, *Wave Propagation in Elastic Solids*, North Holland Series in Applied Mathematics and Mechanics, Vol. 16, H. A. Lauwerier and W. T. Koiter (eds), 1991, Amsterdam, Holland.
44. H. Deresiewicz, 'The effect of boundaries on wave propagation in a liquid-filled porous solid: I. Reflection of plane waves at a free plane boundary (non-dispersive case)', *Bull. Seism. Soc. Am.*, **50**, 599–607 (1960).
45. O. C. Zienkiewicz and R. L. Taylor, *The Finite Element Method.*, Vol. II, 4th edn., McGraw-Hill, New York, 1991.
46. N. M. Newmark, 'A method for computation for structural dynamics', *Proc. ASCE*, **85**, EM1, 67–94 (1959).
47. O. C. Zienkiewicz, 'A further look at Newmark, Houbolt, and other time stepping schemes, A weighted residual approach', *Earthquake Eng. Struct. Dyn.*, **5**, 413–418 1977.